

Finite element comparison between the human and the ovine lumbar intervertebral disc

Gloria Casaroli¹
Tomaso Villa^{2,3}
Fabio Galbusera³

¹ Laboratory of Biological Structures Mechanics, IRCCS Istituto Ortopedico Galeazzi, Milan, Italy

² Laboratory of Biological Structure Mechanics (LaBS), Department of Chemistry, Materials and Chemical Engineering "Giulio Natta", Politecnico di Milano, Milan, Italy

³ Laboratory of Biological Structures Mechanics, IRCCS Istituto Ortopedico Galeazzi, Milan, Italy

Corresponding author:

Gloria Casaroli
Laboratory of Biological Structures Mechanics,
IRCCS Istituto Ortopedico Galeazzi
via Riccardo Galeazzi 4
20161 Milano, Italy
E-mail: gloria.casaroli@grupposandonato.it

Summary

Introduction: Nowadays it is still not clear which loading conditions are responsible for lumbar intervertebral disc failure. Many studies have been conducted to investigate the effect of different loading conditions on the herniation processes, and many of them were based on the ovine model. However, the biomechanical similarities between the human and the ovine lumbar disc have been demonstrated in the main planes only, whereas it is not known if they are comparable under complex loading conditions too. The aim of this study was to compare the mechanical response of the ovine and the human lumbar intervertebral disc under complex loading conditions, in order to investigate differences and similarities between the species.

The loading scenarios described in a finite element study on a human lumbar segment were applied to a model of the ovine disc, and the results were then compared.

It has been shown that combined loads generated highest strains in both the models, and the maximum strains had the same location in the posterior or in the postero-lateral region of the annulus, according to the loading scenario.

Conclusion: The ovine disc can be used in spinal

research to investigate herniation process under any loading conditions.

Level of evidence: V.

KEY WORDS: animal model, finite element analysis, anisotropic hyperelastic.

Introduction

The ovine lumbar intervertebral disc (IVD) is often used as a model to investigate the mechanical behavior of the human lumbar one¹⁻⁴. The acceptance of the ovine model for biomechanical investigations is mainly based on the similar spinal flexibility of the human and the ovine species in the physiological main planes: indeed, both human and ovine spine showed a higher range of motion (ROM) in flexion-extension (FL-EX) and in lateral bending (LB) than in axial rotation (AR)⁵. In the last years, many experimental and numerical studies demonstrated that complex loading conditions favor disc damaging: studies on human specimens demonstrated that the combination of compression with AR, LB and FL caused disc prolapses in the postero-lateral region of the annulus⁶⁻¹⁰. Experimental tests conducted by Adams et al. demonstrated that both the application of compressive loads with forward flexion and complex physiological loads generated damages in the posterior region of the annulus fibrosus, postero-lateral radial fissure, protrusion and posterior nuclear extrusion^{6,7}. They also found that the peaks of stress were largest in the posterior region of the annulus. Edwards et al.⁸ investigated the stress in different regions of the annulus applying a compressive load and different angles of flexion, finding largest stresses located posteriorly. Many numerical studies on the human lumbar disc have been also conducted, confirming the clinical and the experimental outcomes. There are many advantages in using finite element methods: first, it reveals some mechanical parameters that are not always experimentally measurable; second, it allows doing parametric studies in control conditions, which is very useful for biological systems; finally, it permits quicker and cheaper analysis than experimental testing. Lu et al.⁹ conducted a numerical study combining compression, bending and twisting with the fluid diurnal exchange within the disc, finding that all these factors contributed to progressive failure of the annulus, which started in the posterior region at the junction of the disc and the endplate.

Shirazi-Adl et al.¹⁰ investigated the fibers strains under single and combined loads, finding that the maximum strain occurred in the innermost annulus in the postero-lateral region, and then the failure progresses radially to the outer layers.

Recently, Berger-Roscher et al.¹¹ performed an experimental study on sheep lumbar segments investigating the effect of different complex loading scenarios on the generation of failure. They concluded that the combination of FL, LB and AR had a high risk of failure, and FL had a main role in the failure of the IVD. The same loading conditions were investigated by Casaroli et al.¹² in an *in silico* study, demonstrating that the combination of the rotations in the three main planes generated the highest state of stress in the postero-lateral region of the annulus fibrosus.

Despite the ovine model has been used to investigate the effect of many complex load combinations, a direct comparison with the human IVD has been performed under simple loading scenarios only. However, the different geometry, mechanical properties and collagen fiber orientation could lead to a different behavior of the two models. For this reason, we think that an investigation on how the human and the ovine lumbar IVDs react to different complex loading condition is necessary to allow researchers making conclusions on the behavior of the disc under any loading conditions.

The aim of this study was therefore to compare the annular strains generated by complex loading conditions of the ovine lumbar IVD with the human one¹³, using a finite element analysis. A previously developed model of the ovine lumbar IVD has been used for this study¹⁴ and compared to the human model

presented by Schmidt et al.¹³ under the same loading conditions. The hypotheses of the study were that, as in the human IVD, (I) the ovine model underwent the highest strains in the posterior and in the postero-lateral region of the annulus fibrosus, and that (II) complex loading scenarios induced the highest strain and intradiscal pressure values.

Materials and methods

A finite element model of the ovine lumbar IVD¹⁴ and the human model presented by Schmidt et al.¹³ were compared for this investigation and the same loading conditions were applied. The two models had different structural and geometrical properties (Tab. I). For the ovine model, the geometry has been generated by the reconstruction of the cranial and caudal surface of L3-4 vertebral bodies and the disc has been generated using a custom Python script. The model was composed by 56496 hexahedral elements and annulus fibrosus was described as an anisotropic hyperelastic tissue. The mechanical properties of the nucleus pulposus and of the cartilaginous and bony endplates were taken from the literature¹⁵. A convergence analysis based on the flexibility has been performed¹² generating three different mesh sizes (mesh 1 had 4500 elements, mesh 2 56496 elements and mesh 3 had 90816 elements), and the model was then validated comparing the results with the flexibility data measured *in vitro* by Reitmaier et al.¹⁶. Because the rotation difference between the meshes was lower than 5%, mesh 2 has been used for the study. In both studies, the models were constrained

Table I. Structural and geometrical properties of the human and the ovine model investigated in this study.

	Human	Ovine
Spine segment	L4-5	L3-4
Collagen fibers	Spring elements, stress-strain behavior	Anisotropic hyperelastic
Fibers orientation	Ventral = 24°, Dorsal = 46°	Anterior = 29°, Lateral = 30°, Posterior = 28°
Ground substance	Mooney - Rivlin, E = 1.35 MPa	Neo - Hookean
Nucleus pulposus	Mooney - Rivlin, E = 0.9 MPa	Neo - Hookean
Bony endplate	Linear elastic, E = 4000 - 1200 MPa, $\nu = 0.3$	Linear elastic, E=1000 MPa, $\nu = 0.3$
Cartilaginous endplate	Linear elastic, E = 23.8 MPa, $\nu = 0.4$	Linear elastic, E = 24, $\nu = 0.4$
Anterior height	13 mm	4.5 mm
Posterior height	10 mm	2.5 mm
Disc width	51 mm	30 mm
Disc depth	32 mm	22 mm
Nucleus pulposus width	36 mm	20.5 mm
Nucleus pulposus depth	17 mm	9.5 mm

at the caudal endplate in all degree of freedom. In order to transfer the load to the disc, an application node has been defined and attached to the cranial endplate by beam elements. The loading scenarios analyzed by Schmidt consisted in a follower load of 500 N and an unconstrained moment of 7.5 Nm, which corresponds to the physiological ROM; the loading direction was changed of 15 degree between each pair of the three anatomical main-planes (Fig. 1). Because of the different anatomy and physiological loads of the two species, a moment of 3.75 Nm, correspondent to the physiological ROM of sheep, and a follower load of 130 N were applied¹⁶. The resulting load was equivalent to a complex load due to the combination of two main rotations (Fig. 2), which had a different influence according to the rotation angle α . For example, when $\alpha=0^\circ$ a single moment was applied; for $\alpha=15^\circ$ and the reference system was rotating in the transversal (x-y) anatomical plane (Fig. 1), flexion and lateral bending were applied together, but flexion had a dominant component. Instead, when $\alpha=45^\circ$, lateral bending and flexion had the same influence. The simulations were performed in Abaqus 6.14 (Simulia, Dassault Systemes, Providence, RI, USA). Each simulation was composed by two steps: during the first step, the swelling of the nucleus pulposus was simulated generating a pre-stress until a pressure of 0.2 MPa was reached and maintained the added stress constant along the whole simulation. In the second step, the external loads were applied. According to the study of Schmidt, the following parameters were analyzed:

- the ROM in the main directions, as indicator of the disc flexibility;
- the intradiscal pressure (IDP) of the nucleus pul-

posus, because it was assumed that a higher internal pressure combined with disc lesions could facilitate herniation. A set of element in the middle of the nucleus pulposus, and for each element the IDP was calculates as

$$IDP = \frac{\sigma_1 + \sigma_2 + \sigma_3}{3}$$

and the average value was reported.

- the circumferential strains in the annulus, because it was considered an indicator of the strains in the collagen fibers and a predictor of the initiation of fiber breakages;
- the resulting shear strain ϵ_{RS} acting in the transversal plane between the annulus and the cartilaginous endplates, because it was considered to be responsible for the generation of peripheral rim lesions⁴ and endplate junction failures. ϵ_{RS} was calculated as

$$\epsilon_{RS} = \sqrt{\epsilon_{xz}^2 + \epsilon_{yz}^2}$$

where z was the cranio-caudal axis and x-y axes lay in the transversal plane.

Results

In both models, the highest ROM was predicted in FL, followed by EX, LB and AR (Tab. II).

In general, in the ovine model the IDP was higher under complex loads than under the main rotations. The highest value was reached when LB was combined with AR (range 0.6-0.8 MPa), whereas in the human disc the IDP was highest under pure FL (Fig. 3). In

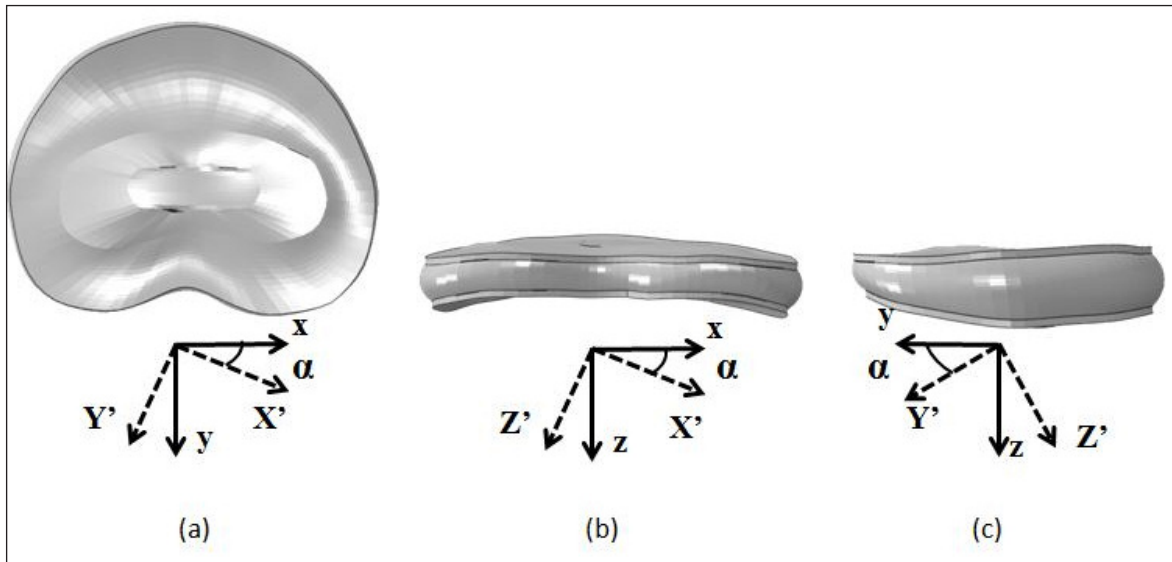


Figure 1. Schematic representation of the reference systems used for the different loading scenarios. For the combination of (a) flexion - extension (FL-EX) and lateral bending (LB), the x and the y axes were incrementally rotated by an α angle of 15 degrees around the z axis; for the combination of (b) FL-EX and axial rotation (AR), the x and the z axes were incrementally rotated by 15 degrees around the y axis; for the combination of (c) AR and LB, the y and the z axes were incrementally rotated by 15 degrees around the x axis.

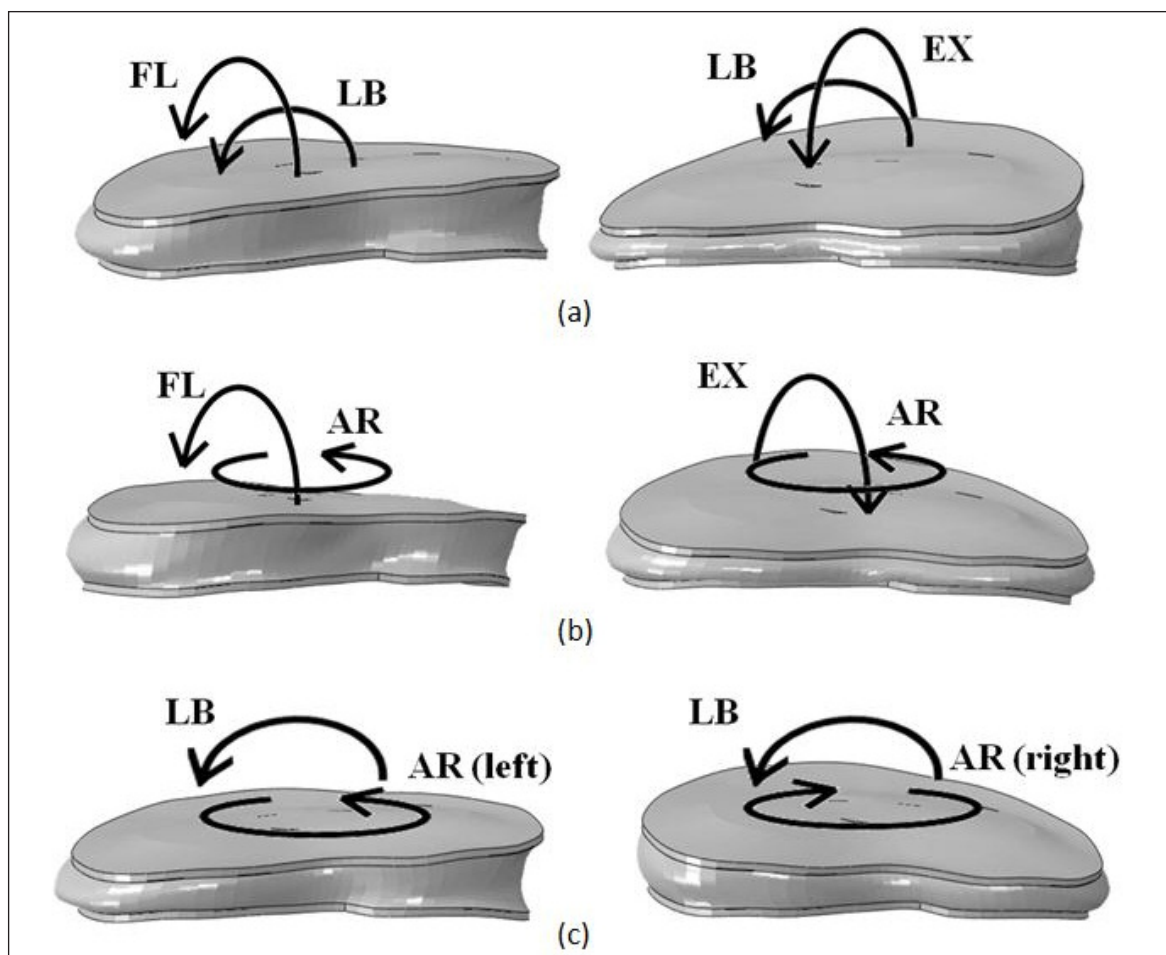


Figure 2. Resulting rotations generated by the combination of (a) flexion-extension (FL-EX) and lateral bending (LB), (b) FL-EX and axial rotation (AR), (c) AR and LB.

Table II. Range of motion in the main planes of the human and of the ovine model under 7.5 and 3.75 Nm.

	ROM (°)	
	Human	Ovine
Flexion	6.0	7.5
Extension	4.3	7.1
Lateral bending	4.5	5.2
Axial rotation	1.8	2.8

the main planes, the IDP of the ovine model was highest in LB (0.69 MPa vs 0.44 MPa in human), followed by AR (0.67 MPa vs 0.57 MPa in human), EX (0.63 MPa vs 0.62 MPa in human) and FL (0.52 MPa vs 0.71 MPa in human).

In the current study, the largest circumferential strain was found under the combination of FL and AR (20%), whereas in the human model the fiber strain was highest under the combination of AR and LB (19.8%) (Fig. 4). In general, the strains had similar trends and were highest under combined loads, ex-

cept in the ovine model under the combination of LB and AR, in which the strain was highest for pure LB (Fig. 4). In both models, the highest strains were located in the posterior and the postero-lateral regions (Fig. 5). In the ovine model, the combination of LB with FL and EX generated the highest strain in the posterior and in the postero-lateral region, respectively (Fig. 5). The combination of FL with AR generated the highest strain in the posterior region in both the models, whereas under EX and AR the strain was highest in the postero-lateral and in the lateral region

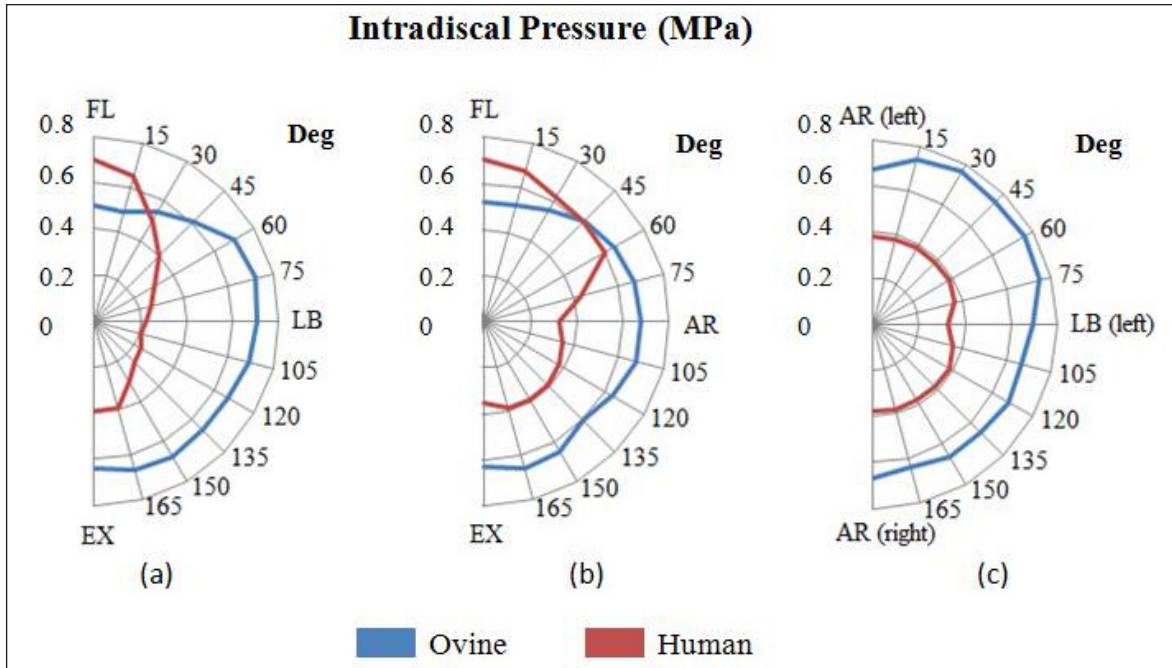


Figure 3. Comparison between the ovine and the human maximum Intradiscal Pressure values under all the applied loading scenarios (adapted from Schmidt et al.⁹). FL means flexion, EX means extension, LB means lateral bending and AR means axial rotation.

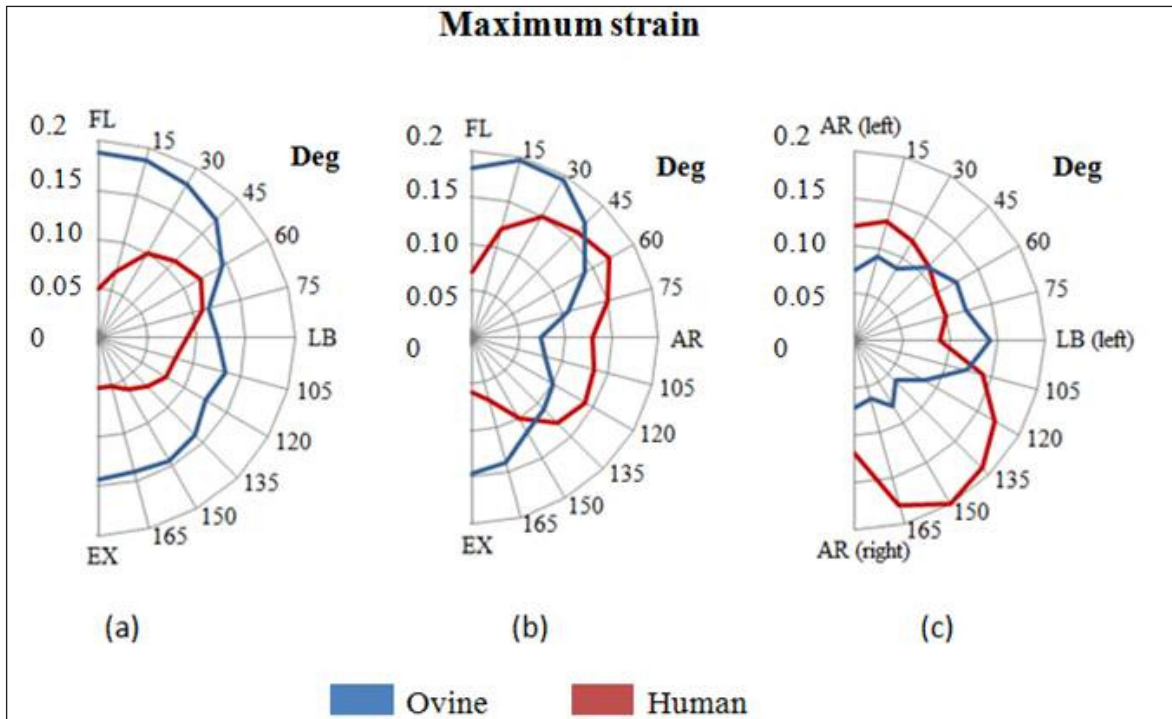


Figure 4. Comparison between the ovine maximum circumferential strain of the annulus fibrosus and the human maximum fiber strains under all the applied loading scenarios (adapted from Schmidt et al.⁹). FL means flexion, EX means extension, LB means lateral bending and AR means axial rotation.

for the ovine and for the human model, respectively. Under the combination of LB and AR the largest strains were located postero-laterally in both the models (Fig. 5).

Regarding the maximum shear strains, the human model was subjected to higher strains than the ovine one, especially under FL-EX + LB (Fig. 6). The highest values were found under the combination of EX

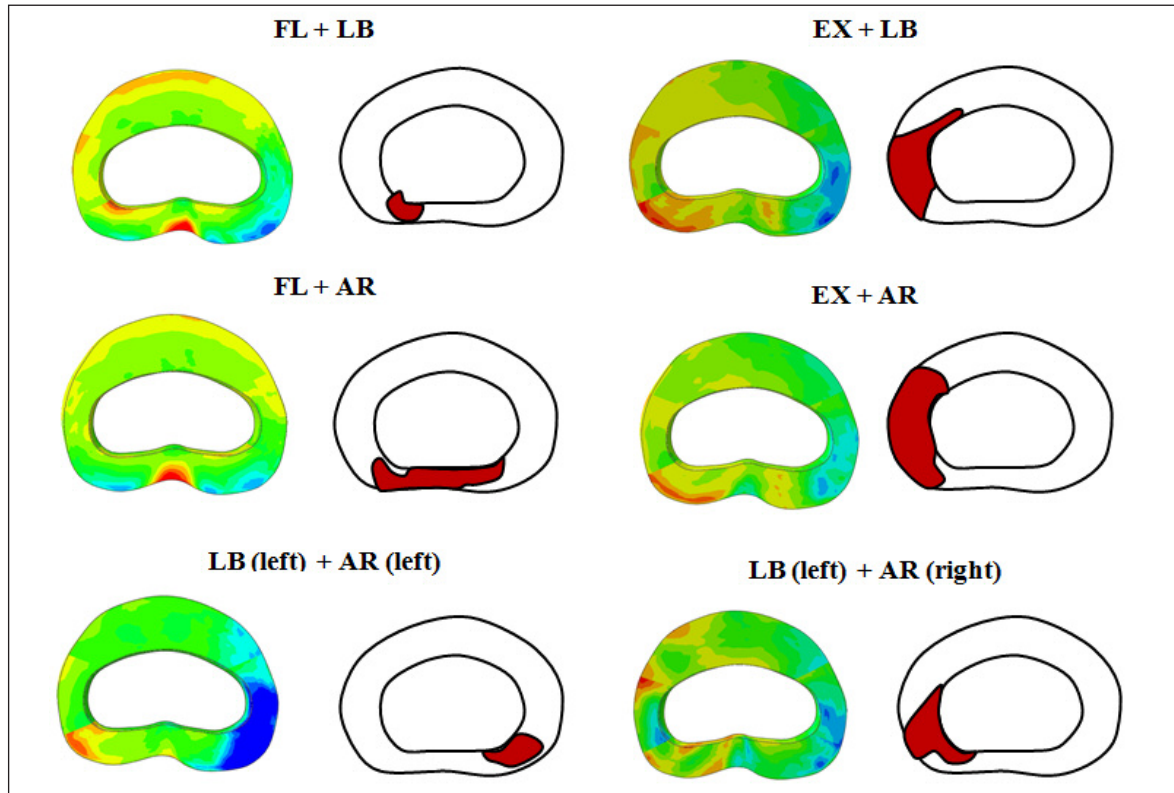


Figure 5. Location of the maximum circumferential strain in the ovine finite element model. The red line includes the area indicated by Schmidt⁹ as characterized by the most strained fibers in the human healthy disc. FL means flexion, EX means extension, LB means lateral bending and AR means axial rotation.

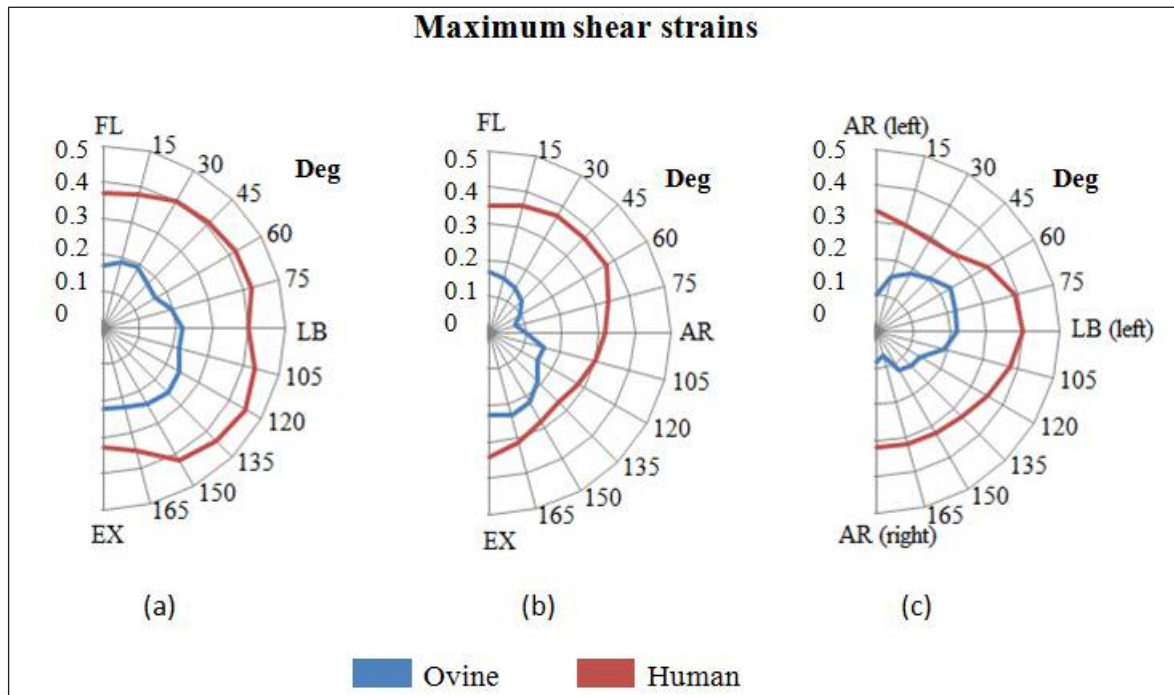


Figure 6. Comparison between the ovine and the human maximum shear strain at the interface between the annulus and the endplate under all the applied loading scenarios (adapted from Schmidt et al.⁹). FL means flexion, EX means extension, LB means lateral bending and AR means axial rotation.

and LB, but they were in general constant, with a difference always lower than 10% under the different loading conditions. The maximum shear strains resulted to be located in the postero-lateral region in both cases when FL-EX was applied, whereas it was lateral under the combination of LB and AR (Fig. 7). Each simulation took around 6 hours to be completed and 39 simulations were done.

Discussion

In this study, a comparative analysis of the mechanical behavior of the human and ovine lumbar IVD under combined loading conditions has been performed. Although the models showed some differences in the maximum shear strain and IDP responses under specific combinations of loads, in both cases FL seemed to keep the disc in an unsafe condition, especially when combined with other loads. Moreover for both models, the maximum strains had the same location in the posterior or in the postero-lateral region of the annulus, according to the applied loading scenario.

The comparison took into account the physiological differences between the species: although the loading scenarios were the same, the entity of the loads applied was lower for the ovine, in order to keep the

discs within their ROM. However, in both the models, the flexibility was highest in FL-EX, followed by LB and AR, and the numerical results were in agreement with *in vitro* findings¹⁷.

The maximum IDP values showed a different behavior between the two models, except that it remained constant under the different combinations of LB and AR. However, the maximum values obtained for the ovine disc were in agreement with experimental values measured by Reitmaier et al.¹⁸. The large differences between the results in the two studies could be due to the geometrical and mechanical properties of the ovine and human nucleus pulposus, but also to the method used to evaluate the maximum IDP value. In both cases, the nucleus was described as a solid material, therefore when it was loaded, a pressure gradient ranging from negative to positive values was generated. In the current analysis, the average of the pressure among a set of elements that were representative of the centre of the nucleus pulposus has been reported in order to reduce the influence of this gradient, whereas it was not clear which values were reported in the reference study. Indeed Adams et al.¹⁹ reported that within the human lumbar nucleus, stresses do not vary along any direction. The two models showed some differences in the maximum strain values; in both models, the maximum strains were lower than 20%, and the highest strains were

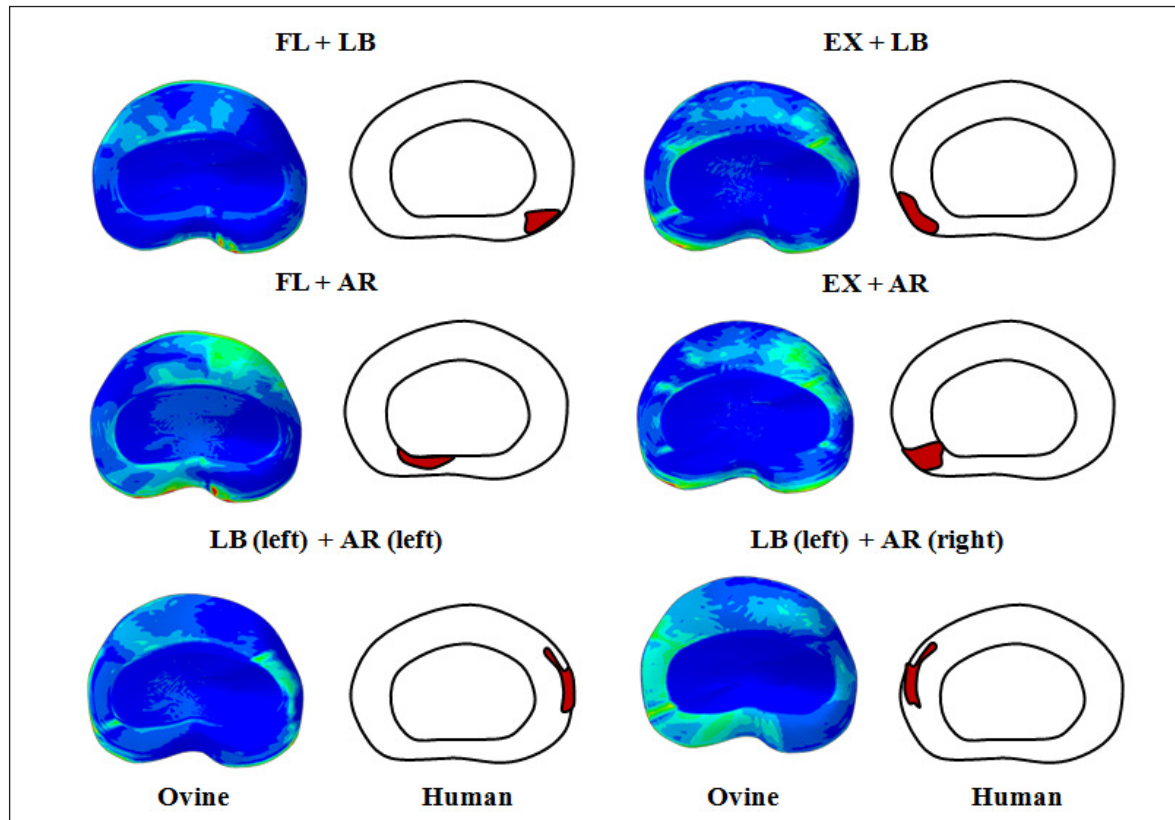


Figure 7. Location of the maximum shear strain in the ovine finite element model. The red line includes the area indicated by Schmidt⁹ as characterized by highest shear strain in the human healthy disc. FL means flexion, EX means extension, LB means lateral bending and AR means axial rotation.

reached when FL was combined with the AR or with the LB, supporting the results that FL has a main role in generating annulus failure. However, the general trends and the location of the maximum strains under different loading conditions were similar, supporting the hypothesis that the ovine lumbar IVD is a good model of the human one for investigating annulus herniation. Indeed, in both the models the largest strains of the annulus occurred in the posterior and in the postero-lateral region, in agreement with *in vitro* and clinical findings²⁰⁻²³. Schmidt et al. did not indicate the location of the maximum strain for each loading scenario, but they only highlighted which region was subjected to the highest strain. However, a direct comparison of the results was not possible due to the different structural properties between the two models. Indeed, in the ovine annulus fibrosus the collagen fibers were not directly represented, and their mechanical effect was due to the definition of the material orientation of the anisotropic tissue. In the human model, the collagen fibers were represented by spring elements, giving the possibility to estimate the strain in the fiber direction. In this study, the circumferential strain of the annulus fibrosus was assumed to be representative of the collagen fibers strains. The maximum shear strains at the interfaces with the cartilaginous endplates were higher in the human model than in the ovine one. Contrary to the fiber strains, the shear strain at the endplates interface was largest under LB + EX than LB + FL, and a peak of strain was reached under LB with a slight AR in the same direction. The maximum values were located in the posterior region and, in the ovine model, the highest values were mainly located at the caudal endplate. In the reference study, this last aspect was not indicated, but it has been clinically demonstrated that in human the occurrence of failure is higher close to the lower surface²⁴.

From a biomechanical point of view, this study confirms that the ovine model is a good surrogate of the human disc for investigating failure. The fact that in both the human and the ovine IVD the location of the maximum strain is the posterior and the postero-lateral region allows the clinical researcher using the ovine model for investigating the mechanical causes of herniation in any loading conditions. Moreover the study suggests that in both species, a component of FL favors the fibers strain and consequently their breakage, whereas in the ovine the AR seems to have more effect on the generation of rim lesions or endplate failures. These results are in agreement with the experimental outcomes of Wade²⁵ and Veres³; on contrast, in the healthy human the influence of each load component on the shear strain is constant. However, the maximum strains were located in the posterior region of the annulus in both species. Other studies reported the most stressed region the postero-lateral one^{9,10, 26-29}: Qasim et al.²⁷ showed that in the human healthy disc the damage started in the posterior annulus and then propagated in the postero-lateral part, identifying FL as the main responsible load for

disc failure. Further numerical studies based on the ovine lumbar model, showed that the inner part of the posterior annulus is the most stressed under complex loading conditions^{12,30}, in agreement with studies on human lumbar disc⁶⁻¹⁰. Based on this consideration, the ovine model is suitable to investigate the generation and the location of failures, whereas more caution is needed to define the specific kind of failure. However, it is not directly be used for patient specific application. The advantage of having a good animal model is related to research and to the industry, or to surgical training. Hence, for this kind of applications the model is feasible because it allows having results in few hours. On the other hand, the method used for generating the ovine model could be used for generating patient specific models. The creation of the geometry was semi-automatic¹⁴ and the mesh could be improved to make the simulation quicker. If it was assumed to have a dataset of material properties for different degrees of degeneration of the human disc, any models could be created and many simulations can be performed in a short time (few hours), that may be compatible with the pre-recovery period.

This study has some limitations. First, the human model used for the comparison included the posterior elements and the ligaments, which protect the disc by limiting the movements. In particular, the facet joints constrain the AR, therefore the moment that is transferred to the disc is lower than the applied moment. Second, it was assumed that the circumferential strain was representative of the collagen fiber strains: in the ovine model, the collagen fiber had an orientation of 28, 30 and 29 degrees in the posterior, lateral and anterior region respectively, since the axial component of the strain should be considered.

The effect of the different geometry on the mechanical response of the disc has not been investigated. This could be done applying the same material properties to the two models. However, it has been already demonstrated by Schmidt and Reitmaier³¹ that the geometrical parameters have a great influence on the mechanical behavior of the disc. They investigated the effect of the geometry and of some biological and mechanical parameters, adopting the ovine model to the human one. Tissue degeneration was not investigated. The reason is that data on the degenerated tissues of sheep are lacking and they are not easy to obtain, due to the unavailability of degenerated specimens. These limitations could be overcome in order to make the model more feasible to clinical application. First of all, the vertebral bodies, the posterior structures and the ligaments may be included in the ovine model and a step-wise comparison of the disc flexibility with the human disc should be performed. By a clinical point of view, this analysis could improve the knowledge of the disc behavior in different clinical conditions. Moreover, a parametric study on the anatomy and on the mechanical properties of the disc should be performed, as well as an investigation on the influence of the hydration of the nucleus, in order to better simulate pathological situations.

Conclusion

In this study a comparison of the mechanical response to complex loads between the human and the ovine lumbar IVD has been performed. The study highlighted some differences and some important similarities between the mechanical behavior of the ovine and human lumbar IVD. The ovine model is largely used in biomechanical experiments under any scenarios as a surrogate of the human IVD, so it is important for researchers to know if the behavior is comparable to the human one in any loading conditions. Here, it has been demonstrated that the human and the ovine models have some similarities in the strain fields of the annulus fibrosus, and that the maximum strain is in general located in the posterior region of the disc.

Ethics

The Authors declare that this research was conducted following basic ethical aspects and international standards as required by the journal and recently update in³².

Conflict of interest

None.

References

- Veres SP, Robertson PA, Broom ND. The morphology of acute disc herniation: a clinically relevant model defining the role of flexion. *Spine (Phila Pa 1976)*. United States. Oct 2009;34(21):2288-2296.
- Veres SP, Robertson PA, Broom ND. ISSLS prize winner: microstructure and mechanical disruption of the lumbar disc annulus: part II: how the annulus fails under hydrostatic pressure. *Spine (Phila Pa 1976)*. Dec 2008;1;33(25):2711-2720. Available from: <http://www.ncbi.nlm.nih.gov/pubmed/19002077>
- Veres SP, Robertson PA, Broom ND. The influence of torsion on disc herniation when combined with flexion. *Eur Spine J*. Sep 2010;19(9):1468-1478. Available from: <http://www.pubmedcentral.nih.gov/articlerender.fcgi?artid=2989279&tool=pmcentrez&rendertype=abstract>
- Osti OL, Vernon-Roberts B, Fraser RD. Anulus Tears and Intervertebral Disc Degeneration. An experimental Study Using an Animal Model. *Spine*. 1990;762-767.
- Wilke H-J, Kettler A, Claes L. Are Sheep Spines a Valid Biomechanical Model for Human Spines?. 1997:2365-2374. Available from: <http://www.ncbi.nlm.nih.gov/pubmed/9355217>
- Adams MA, Freeman BJ, Morrison HP, Nelson IW, Dolan P. Mechanical initiation of intervertebral disc degeneration. *Spine (Phila Pa 1976)*. United States; 2000 Jul;25(13):1625-36.
- Adams MA, Hutton WC. The mechanics of prolapsed intervertebral disc. *Int Orthop*. Germany. 1982;6(4):249-253.
- Edwards WT, Ordway NR, Zheng Y, McCullen G, Han Z, Yuan HA. Peak stresses observed in the posterior lateral anulus. *Spine (Phila Pa 1976)*. United States. Aug 2001;26(16):1753-1759.
- Lu YM, Hutton WC, Gharpuray VM. Do bending, twisting, and diurnal fluid changes in the disc affect the propensity to prolapse? A viscoelastic finite element model. *Spine (Phila Pa 1976)*. United States. Nov 1996;21(22):2570-2579.
- Shirazi-Adl A. Strain in fibers of a lumbar disc. Analysis of the role of lifting in producing disc prolapse. *Spine (Phila Pa 1976)*. United States. Jan 1989;14(1):96-103.
- Berger-Roscher N, Casaroli G, Rasche V, Villa T, Galbusera F, Wilke H-J. Influence of Complex Loading Conditions on Intervertebral Disc Failure. *Spine (Phila Pa 1976)*. 2016.
- Casaroli G, Villa T, Bassani T, Berger-Roscher N, Wilke H-J, Galbusera F. Numerical Prediction of the Mechanical Failure of the Intervertebral Disc under Complex Loading Conditions. *Materials (Basel)*. 2017;10(1):31. Available from: <http://www.mdpi.com/1996-1944/10/1/31>
- Schmidt H, Kettler A, Rohlmann A, Claes L, Wilke H-J. The risk of disc prolapses with complex loading in different degrees of disc degeneration - a finite element analysis. *Clin Biomech (Bristol, Avon)*. Nov 2007;22(9): 988-998. Available from: <http://www.ncbi.nlm.nih.gov/pubmed/17822814>
- Casaroli G, Galbusera F, Jonas R, Schlager B, Wilke H-J, Villa T. A Novel Finite Element Model of the Ovine Lumbar Intervertebral Disc with Anisotropic Hyperelastic Material Properties. *PLoS One*. 2017;1-15.
- Ayturk UM, Gadomski B, Schuldt D, Patel V, Puttlitz CM. Modeling degenerative disk disease in the lumbar spine: a combined experimental, constitutive, and computational approach. *J Biomech Eng [Internet]*. [cited 2014 Nov 11] Oct 2012;134(10):101003-1-11. Available from: <http://www.ncbi.nlm.nih.gov/pubmed/23083194>
- Reitmaier S, Volkheimer D, Berger-Roscher N, Wilke H-J, Ignatius A. Increase or decrease in stability after nucleotomy? Conflicting in vitro and in vivo results in the sheep model. *J R Soc Interface*. 2014;11(100):20140650. Available from: <http://eutils.ncbi.nlm.nih.gov/entrez/eutils/elink.fcgi?dbfrom=pubmed&id=25209401&retmode=ref&cmd=prlinks>
- Reitmaier S, Volkheimer D, Berger-Roscher N, Wilke H, et al. Increase or decrease in stability after nucleotomy? Conflicting in vitro and in vivo results in the sheep model. *JR Soc Interface*. 2014;11. Available from: <http://dx.doi.org/10.1098/rsif.2014.0650>
- Reitmaier S, Schmidt H, Ihler R, Kocak T, Graf N, Ignatius A, et al. Preliminary investigations on intradiscal pressures during daily activities: An in vivo study using the merino sheep. *PLoS One* Jan 2013;8(7):e69610. Available from: <http://www.pubmedcentral.nih.gov/articlerender.fcgi?artid=3722231&tool=pmcentrez&rendertype=abstract>
- Adams MA, Nally DSMC, Dolan P. "Stress" distributions inside intervertebral discs. The effects of age and degeneration. 1992;965-972.
- Berger-Roscher N, Casaroli G, Rasche V, Villa T, Galbusera F, Wilke HJ. Influence of Complex Loading Conditions on Intervertebral Disc Failure. *Spine (Phila Pa 1976)*. 2017 Jan 15;42(2):E70-E85.
- Rajasekaran S, Bajaj N, Tubaki V, Kanna RM, Shetty AP. ISSLS Prize Winner. *Spine (Phila Pa 1976)*. 2013;38(17): 1491-500. Available from: <http://www.ncbi.nlm.nih.gov/pubmed/23680832>
- Ebeling U, Reulen HJ. Are there typical localisations of lumbar disc herniations? A prospective study. *Acta Neurochir (Wien)*. Austria. 1992;117(3-4):143-148.
- Spangfort EV. The lumbar disc herniation. A computer-aided analysis of 2,504 operations. *Acta Orthop Scand Suppl*. Sweden. 1972;142:1-95.

24. Rajasekaran S, Bajaj N, Tubaki V, Kanna RM, Shetty AP. ISSLS Prize winner: The anatomy of failure in lumbar disc herniation: an in vivo, multimodal, prospective study of 181 subjects. *Spine (Phila Pa 1976)* 1 Aug 2013;38(17):1491-1500. Available from: <http://www.ncbi.nlm.nih.gov/pubmed/23680832>
25. Wade KR, Robertson PA, Thambyah A, Broom ND. How Healthy Discs Herniate. *Spine (Phila Pa 1976)*. 2014;39(13):1018-1028. Available from: <http://content.wkhealth.com/linkback/openurl?sid=WKPTLP:landingpage&an=00007632-201406010-00006>
26. Holzapfel GA, Schulze-Bauer CAJ, Feigl G, Regitnig P. Single lamellar mechanics of the human lumbar annulus fibrosus. *Biomech Model Mechanobiol*. 2005;3:125-140.
27. Qasim M, Natarajan RN, An HS, Andersson GBJ. Initiation and progression of mechanical damage in the intervertebral disc under cyclic loading using continuum damage mechanics methodology: A finite element study. *J Biomech*. Elsevier. [cited 2014 Dec 3] 26 Jul 2012;45(11):1934-1940. Available from: <http://www.pubmedcentral.nih.gov/articlerender.fcgi?artid=3787695&tool=pmcentrez&render-type=abstract>
28. Reutlinger C, Bürki A, Brandejsky V, Ebert L, Büchler P. Specimen specific parameter identification of ovine lumbar intervertebral discs: On the influence of fibre-matrix and fibre-fibre shear interactions. *J Mech Behav Biomed Mater*. 2014;30:279-289.
29. Skaggs DL, Weidenbaum M, Iatridis JC, Ratcliffe A, Mow VC. Regional variation in tensile properties and biochemical composition of the human lumbar annulus fibrosus. *Spine*. 1994;13:10-1319.
30. Casaroli G, Galbusera F, Villa T. Investigation of the state of stress generated by high loads in the ovine lumbar intervertebral disc using a new anisotropic hyperelastic model. In: Gefen A, Weihs D, editors. *Computer Methods in Biomechanics and Biomedical Engineering Lecture Notes in Bioengineering*. Springer, Cham. 2018:107-113.
31. Schmidt H, Reitmaier S. Is the ovine intervertebral disc a small human one? A finite element model study. *J Mech Behav Biomed Mater*. Elsevier. 2013;17:229-241. Available from: <http://dx.doi.org/10.1016/j.jmbbm.2012.09.010>
32. Padulo J, Oliva F, Frizziero A, Maffulli N. *Muscles, Ligaments and Tendons Journal - Basic principles and recommendations in clinical and field science research: 2016 update*. MLTJ. 2016;6(1):1-5.